

An inductor-free realization of the Chua's circuit based on electronic analogy

Ronilson Rocha · Rene O. Medrano-T.

Received: 5 March 2008 / Accepted: 22 July 2008 / Published online: 20 August 2008
© Springer Science+Business Media B.V. 2008

Abstract Although literature presents several alternatives, an approach based on the electronic analogy was still not considered for the implementation of an inductor-free realization of the double scroll Chua's circuit. This paper presents a new inductor-free configuration of the Chua's circuit based on the electronic analogy. This proposal results in a versatile and functional inductorless implementation of the Chua's circuit that offers new and interesting features for several applications. The analogous circuit is implemented and used to perform an experimental mapping of a large variety of attractors.

Keywords Chaotic system · Electronic analogy · Inductorless Chua's circuit · Experimental attractors

1 Introduction

Numerous natural and artificial systems, completely described by deterministic dynamic laws and nonlin-

ear differential equations without stochastic components, present an unpredictable and apparently random dynamical behavior extremely sensitive to initial conditions. They are known as chaotic systems, and have been studied by mathematicians, physicians, engineers and, more recently, specialists in information and social sciences. These systems present several interesting properties that have a great potential for commercial and industrial applications in several areas, such as engineering, computation, communication, chemistry, medicine, biology, management, finance, electronics consumers, information processing, etc. [1–3].

Experimental activities involving chaotic systems play a very important role to understand theoretical concepts. However, an experimental implementation of a chaotic system can meet various challenges related to the inherent difficulties to build the real system, such as space limitations, precision, financial support, availability of components, etc. In general, a commercial experimental kit tends to be relatively expensive or very qualitative [4]. Thus, the study of chaos in nonlinear electronic circuits has been a very active topic of research.

One of the most important chaotic circuits was created by Leon O. Chua in 1983, which is characterized by its simplicity, easy implementation, robustness and a simple static nonlinearity that allows for a large and diverse set of dynamical behaviors. The Chua's circuit is an autonomous system composed of a network of linear passive elements, connected to a nonlinear

R. Rocha (✉)
Federal University of Ouro Preto—UFOP/EM/DECAT,
Campus Morro do Cruzeiro, 35400-000, Ouro Preto, MG,
Brazil
e-mail: rocha@em.ufop.br

R.O. Medrano-T.
University of São Paulo—USP/Institute of Physics,
C-P: 66318, 05508-900, São Paulo, SP, Brazil
e-mail: rmedrano@if.usp.br

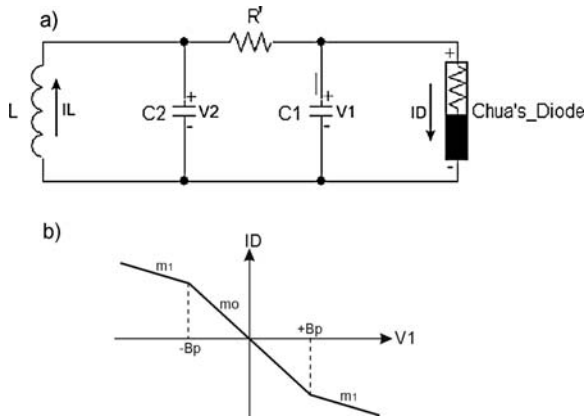


Fig. 1 The schematic Chua's circuit: **a** The Chua's circuit and **b** Characteristic of Chua's diode

active component, whose standard form is shown in Fig. 1a. The linear resistor R' couples a lossless resonant circuit, consisting of a parallel combination of the inductor L and the capacitor C_2 , to a parallel circuit combination of the capacitor C_1 with an active component that behaves as a power source. This component, known as Chua's diode, has a nonlinear negative resistance characteristic. In spite of its simplicity, this system presents a very rich dynamical behavior as: fixed point, Hopf, periodic, period doubling, homoclinic bifurcations, or chaotic attractors [5, 6]. From Fig. 1a, the dynamics of the Chua's circuit can be described by three-coupled first-order nonlinear differential equations:

$$\begin{aligned} \frac{dv_1}{dt} &= -\frac{v_1 - v_2}{R'C_1} - \frac{i_D(v_1)}{C_1}, \\ \frac{dv_2}{dt} &= \frac{v_1 - v_2}{R'C_2} - \frac{i_L}{C_2}, \\ \frac{di_L}{dt} &= -\frac{v_2}{L}, \end{aligned} \tag{1}$$

where $i_D(v_1)$ is the function for the Chua's diode. Although this component can be represented by any scalar function of one variable, generally it is a three-segmented piecewise linear curve shown in Fig. 1b, given by

$$i_D(v_1) = m_0 v_1 + \frac{1}{2}(m_1 - m_0)(|v_1 + B_p| - |v_1 - B_p|), \tag{2}$$

which is chosen for convenience in synthesizing the physical circuit [7]. This set of differential equations

can be simplified through an adequate re-scaling of the variables, which allows for the reduction of the parameters involved in the problem without changing the system dynamics. Defining new variables as:

$$\begin{aligned} x &= \frac{v_1}{B_p}, \quad y = \frac{v_2}{B_p}, \quad z = \frac{R'i_L}{B_p}, \quad \text{and} \\ \tau &= \frac{t}{R'C_2}. \end{aligned}$$

Equations (1) can be described in their dimensionless form as:

$$\begin{aligned} \frac{dx}{d\tau} &= \alpha[-x + y - i_{DN}(x)], \\ \frac{dy}{d\tau} &= x - y + z, \\ \frac{dz}{d\tau} &= -\beta y, \end{aligned} \tag{3}$$

with

$$i_{DN}(x) = a_0 x + \frac{1}{2}(a_1 - a_0)(|x + 1| - |x - 1|), \tag{4}$$

where the new parameters are given by:

$$\begin{aligned} \alpha &= \frac{C_2}{C_1}, \quad \beta = \frac{R'^2 C_2}{L}, \quad a_0 = R'm_0, \quad \text{and} \\ a_1 &= R'm_1. \end{aligned}$$

The success of an experimental implementation of a Chua's circuit basically depends on the realization of the nonlinear element. Several configurations are presented in literature to approach Chua's diode using circuit elements, such as diodes [8], transistors [9], conventional voltage op amps (VOA) [10, 11], current feedback op amps (CFOA) [12, 13] and OTAs [14]. Another critical element in the implementation of a Chua's circuit is the inductor. Since commercial inductance values do not cover a very wide range, the inductor is assembled separately in most applications, resulting in a component having low accuracy and generally large dimensions when compared to other circuit elements. Furthermore, the internal resistance of the inductor can compromise the correct operation of the circuit. Many alternatives to replace the physical inductor in an implementation of a Chua's circuit have been presented in literature, such as the use

of Wien-bridge [15] and inductance emulator circuits based on transistors [16], VOAs [17], CFOAs [12], OTAs [18, 19] and FTFN [20]. A comparative investigation about the configurations of Chua's diode and inductance emulators, as well the combination of them to obtain an inductorless Chua's circuit, is presented in [21].

Although literature presents several alternatives for the implementation of an inductor-free realization of a Chua's circuit, an approach based on the electronic analogy had not yet been considered. Since the dynamics of the Chua's circuit is governed by a set of differential equations, it can be electronically emulated by an analogous electronic circuit based on weighted analog integrators [22]. The nonlinear function of Chua's diode can be approached by line segments generated by polarized diodes in an inverter amplifier. However, a direct electronic implementation of a Chua's circuit from an analogous electronic circuit can be relatively difficult, since the electrical signals are submitted to rigid amplitude and frequency constraints.

This paper presents a new inductor-free configuration of a Chua's circuit based on the electronic analogy. This proposal results in a versatile and functional inductorless implementation for a Chua's circuit that offers new and interesting features for several applications. The analogous circuit reproduces accurately the dynamical behavior of the Chua's circuit, and its parameters can be varied in a large range, including negative values. The three state variables of the analogous Chua's circuit are accessible and available as analog voltage signals. The amplitude and frequency of these signals can be matched according to application, allowing the circuit design for operations with slow dynamics, as required for control purposes, or extremely fast oscillations, in order to create appropriate circuits for use in chaos-based communications. The analogous circuit is implemented and used to perform an experimental mapping of a large variety of attractors, where the perfect match between experiment and simulations can be observed.

2 Analogous Chua's circuit

The design of the analogous Chua's circuit herein, is based on the methodology described in [22]. The sim-

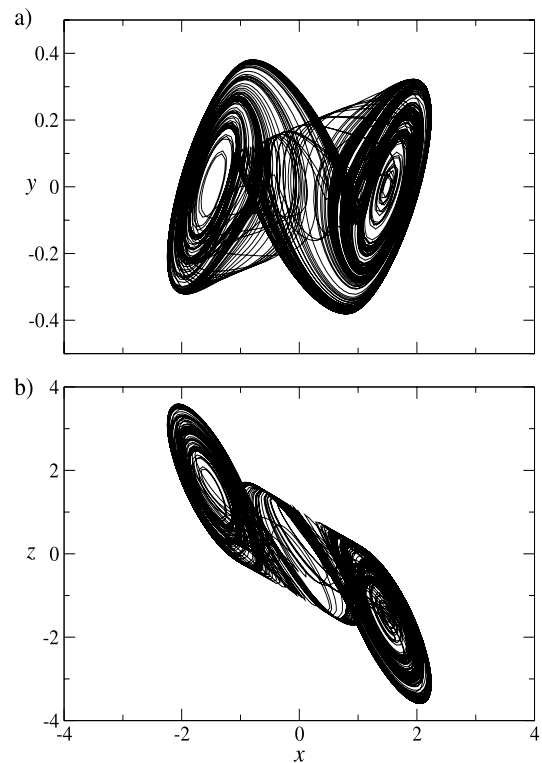


Fig. 2 Projections of the chaotic double-scroll attractor in the Chua's circuit: **a** $(y) \times (x)$ and **b** $(z) \times (x)$

plified Chua's circuit described in (3) is simulated, aiming to estimate the maximum amplitudes of the output signals. Considering $\alpha = 14$, $\beta = 27$ and the Chua's diode characteristic as a three-segment piecewise linear curve with $a_0 = -8/7$ and $a_1 = -5/7$, the chaotic double-scroll attractor obtained in this simulation is presented in Fig. 2, where it can be verified that maximum amplitudes of the variables are $|x_{\max}| = 2.3$ V, $|y_{\max}| = 0.4$ V and $|z_{\max}| = 3.6$ V.

2.1 Redefining the operational range

Since the maximum values for the system variables do not surpass the voltage limits imposed by an usual power supply of ± 12 V, a direct electronic implementation is possible. However, the amplitude of the double-scroll attractor will be extended to ± 5 V, since this value can be considered adequate to minimize the effects of the noises and to allow a comfortable observation of the circuit signals in the oscilloscopes and acquisition systems. Applying the amplitude scaling

in (3), new variables are defined as

$$\bar{x} = 2.2x, \quad \bar{y} = 12.5y, \quad \text{and} \quad \bar{z} = 1.4z,$$

resulting in the following scaled system:

$$\begin{aligned} \dot{\bar{x}} &= \alpha[-\bar{x} + 0.176\bar{y} - \bar{i}_{DN}(\bar{x})], \\ \dot{\bar{y}} &= 5.682\bar{x} - \bar{y} + 8.929\bar{z}, \\ \dot{\bar{z}} &= -0.112\beta\bar{y}, \end{aligned} \tag{5}$$

where the scaled Chua's diode function $\bar{i}_{DN}(\bar{x})$ is given by:

$$\bar{i}_{DN}(\bar{x}) = a_0\bar{x} + \frac{1}{2}(a_1 - a_0)(|\bar{x} + 2.2| - |\bar{x} - 2.2|). \tag{6}$$

Aiming to avoid for any intermediate signal to surpass the voltage limits, it is advisable to normalize the parameter system, dividing the equation system (5) by the value of the greatest parameter. This procedure only implies in a reduction or increase of the system speed and does not affect the final electronic implementation of the analogous Chua's circuit. Considering a reference value of 35 for the greatest parameter in the circuit design, the normalized set of equations of this circuit is given by:

$$\begin{aligned} \dot{\bar{x}} &= a[-\bar{x} + 0.176\bar{y} - \bar{i}_{DN}(\bar{x})], \\ \dot{\bar{y}} &= 0.162\bar{x} - 0.029\bar{y} + 0.255\bar{z}, \\ \dot{\bar{z}} &= -0.112b\bar{y}, \end{aligned} \tag{7}$$

where $a = \alpha/35$ and $b = \beta/35$. Although the value 35 has been stipulated as the reference for the system normalization, it does not represent the superior limit for α and β . Thus, the normalized parameters a and b can be larger than unity and, since these parameters represent voltage gains in the analogous circuit, their maximum values are determined by the saturation thresholds of the components involved in experimental implementation.

2.2 Electronic cells

Since the dynamics of the Chua's circuit is described by a set of three first-order differential equations, the main cell of an analogous electronic circuit is the analog-inverting weighted integrator with operational amplifier, whose transfer function is given by:

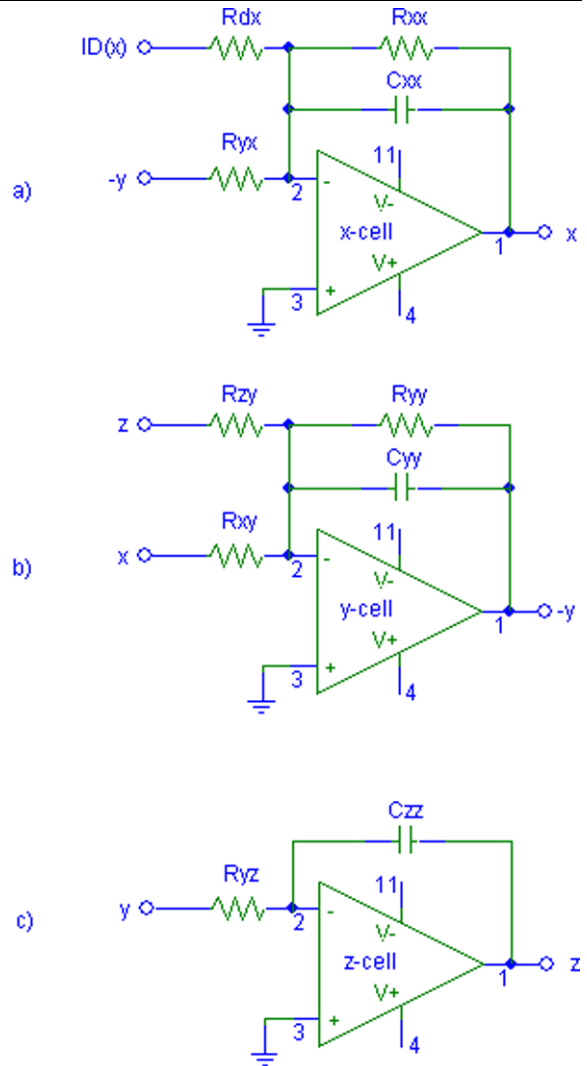


Fig. 3 Electronic implementations of each first-order differential equation of the analogous Chua's circuit: **a** x cell, **b** y cell, and **c** z cell

$$v_o = -\frac{1}{RC} \int \left(\frac{v_x}{R_{x*}} + \frac{v_y}{R_{y*}} + \frac{v_z}{R_{z*}} \right) dt, \tag{8}$$

where v_o is the output voltage, v_x , v_y , and v_z are the input voltages and R_{x*} , R_{y*} , and R_{z*} are the normalized values of the input resistances p.u. (per unity). The dynamics of the analogous circuit are determined by the base resistance R and the integrator capacitance C . The electronic implementation of each first-order differential equation of a scaled Chua's circuit is shown in Fig. 3. A comparison between the integrator transfer function and a normalized first-order differential equation shows that the p.u. values of the input

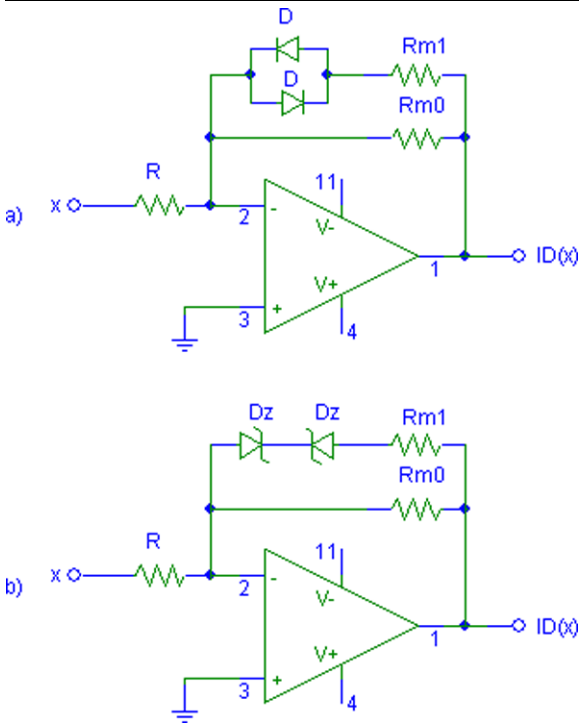


Fig. 4 Analogous Chua's diode implementations: **a** Anti-parallel connection with rectifier or LED diodes and **b** Anti-series connection with zeners diodes

resistances correspond to the inverse of the respective differential equation coefficients.

Another important electronic cell for the implementation of the analogous Chua's circuit is Chua's diode, whose analogous electronic diagrams are presented in Fig. 4. The three-segmented piecewise linear function of Chua's diode is created using an inverter amplifier based on an operational amplifier, whose gain is switched at transition point B_p by diodes in anti-parallel (rectifiers or LEDs) or anti-series (zeners) connections. When the output voltage $i_D(x)$ is within the range $\pm B_p$, both diodes are blocked and the gain of the inverter amplifier is given by $a_0 = R_{m0}/R$. However, if the output voltage $i_D(x)$ is outside of the range $\pm B_p$, one of the diodes is switched on, putting the resistor R_{m1} in parallel with R_{m0} and reducing the gain of the inverter amplifier to

$$a_1 = \frac{R_{m0} \parallel R_{m1}}{R} = \frac{R_{m0} R_{m1}}{R(R_{m0} + R_{m1})}. \tag{9}$$

2.3 The analogous Chua's circuit with fixed parameters

The analogous Chua's circuit that reproduces the normalized three-coupled first-order nonlinear differential equations of the Chua's circuit (7) is obtained by the adequate connection of the individual electronic cells and analogous Chua's diode, as shown in Fig. 5. An extra inverting amplifier is used to transmit a compatible polarity of the signal from the y-cell to the z-cell. All resistances in this analogous circuit are normalized in relation to a base resistance R , which establishes the circuit dynamics together with integrator capacitor value C . Since the voltage drop of a blue LED is approximately 2.2 V, it is used in an anti-parallel diode configuration of the analogous Chua's diode. This effect could be also obtained with the association of three-series rectifier diodes. Considering $a = 0.4$ and $b = 0.771$, the experimental implementation of this circuit is realized using ICs TL071 (single op-amp) and TL074 (quad op-amp). All capacitors are 4.7 nF and the base resistance is 10 kΩ. This analogous electronic implementation that represents the equation system given by (7) successfully reproduces the dynamical behavior of the Chua's circuit. The projections of the attractor obtained by this experimental implementation, observed in a 20 MHz analog oscilloscope on X–Y mode, are shown in Fig. 6. The attractor amplitudes are restricted within the ± 5 V range, indicating that the signals do not surpass the designed limits.

3 Analogous Chua's circuit with variable parameters

The dynamical behavior of the Chua's circuit consists of a rich scenario formed by several types of bifurcations, homoclinic orbits, and stranger attractors, having a great amount of distinct periodic and chaotic attractors which can be observed when the parameters of this circuit are varied. A dimensionless analysis shows that several parameter configurations are completely equivalent, and the seven original parameters of this circuit ($R', C_1, C_2, L, m_0, m_1$ and B_p) can be jointed into only four dimensionless groups (α, β, a_0 and a_1). Admitting fixed parameters for Chua's diode, the analogous Chua's circuit can be easily adapted to allow explicit variations of the dimensionless parameters α

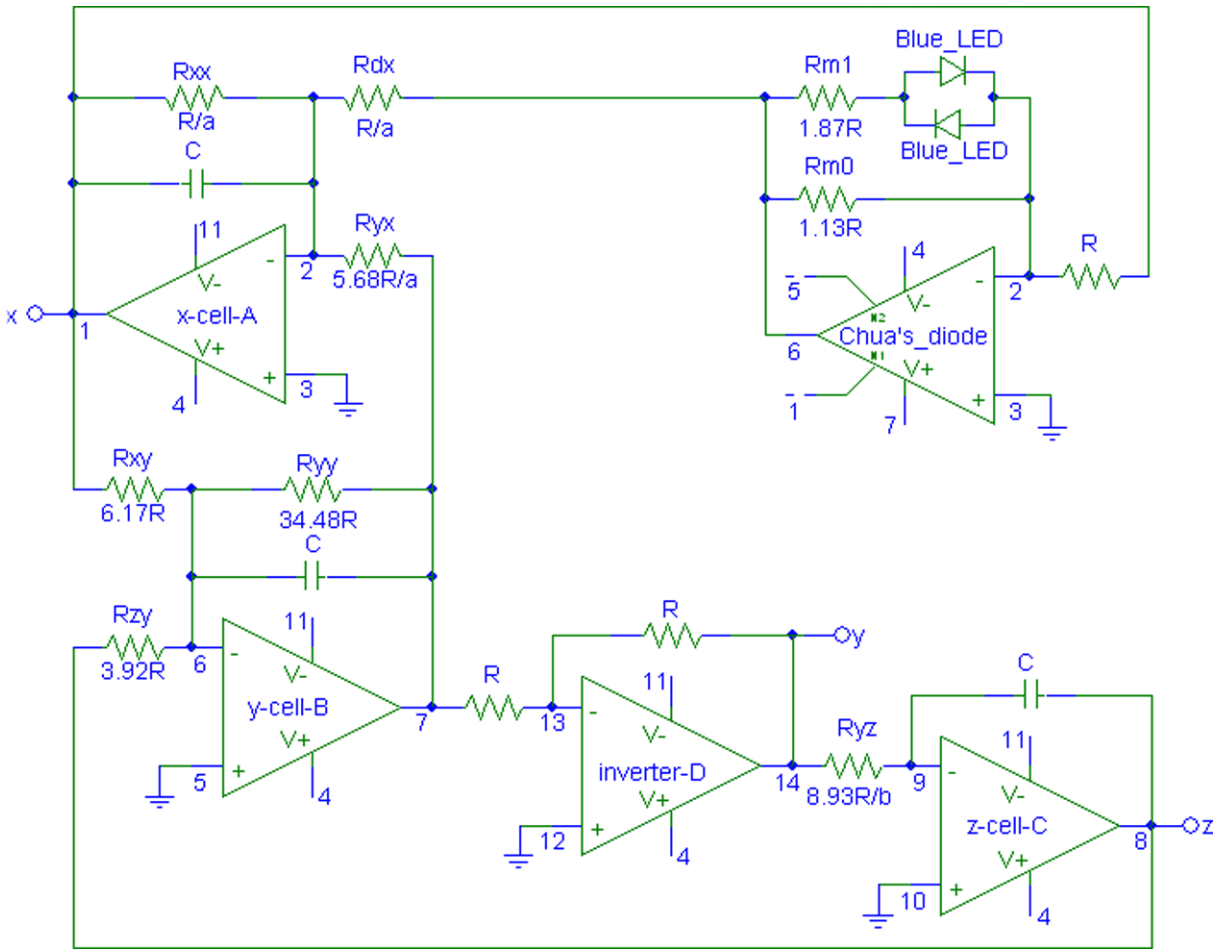


Fig. 5 Analogous Chua's circuit with fixed parameters



Fig. 6 Experimental projections of double-scroll attractor of the analogous Chua's circuit: **a** $(y) \times (x)$ and **b** plane $(z) \times (x)$

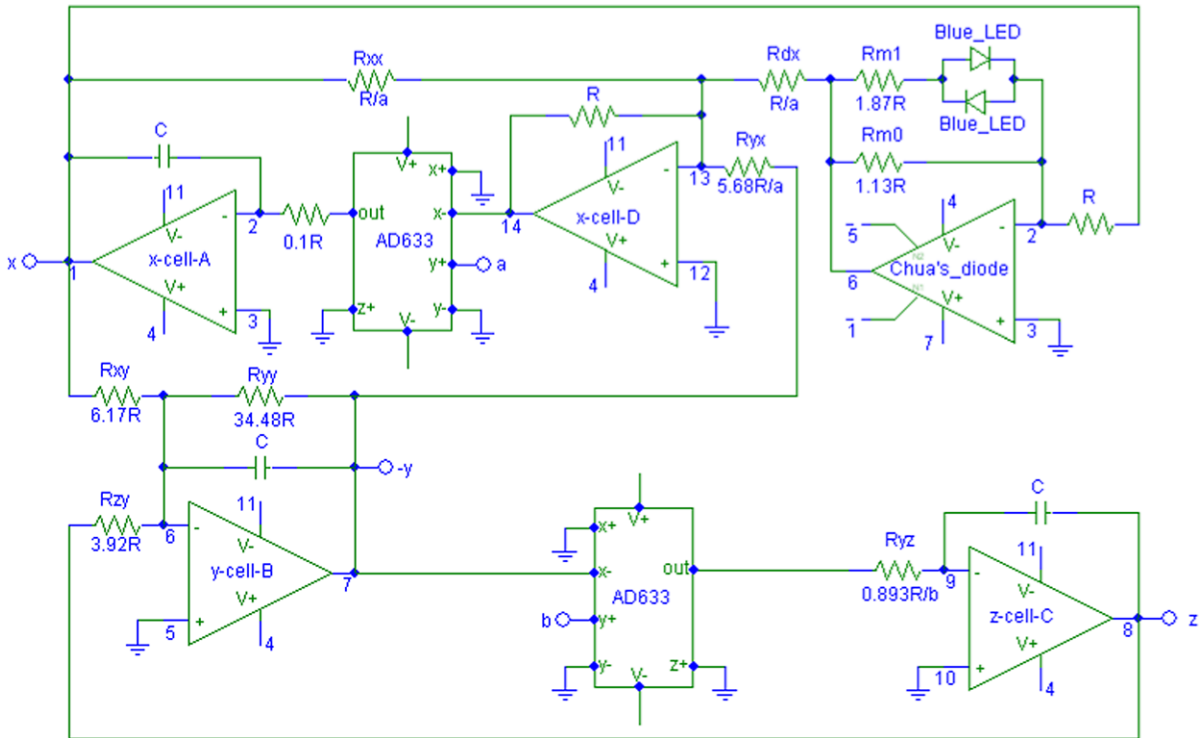


Fig. 7 Analogous Chua's circuit with variable parameters

and β by putting a variable capacitor in x -cell and replacing the resistor R_{yz} by a potentiometer in z -cell, respectively.

Another option for this circuit with variable parameters is shown in Fig. 7, where the x -cell and z -cell are modified. In the x -cell, the derivative of x is initially obtained from a summer, multiplied by $a = \alpha/35$ using an analog multiplier and integrated in an analog weighted integrator to obtain the variable x . In the z -cell, the variable y (a derivative of z) is first multiplied by $b = \beta/35$ and then integrated in an analog integrator to obtain the variable z . The dynamics of this circuit is still described by (7). This version of the analogous Chua's circuit with variable parameters allows for the normalized dimensionless parameters a and b to be represented by external DC voltage levels, which become easy-to-execute parameter variations when a computer with acquisition board with analog outputs is used. The experimental implementation of the analogous Chua's circuit with variable parameters is realized using the ICs AD633 (analog multiplier), TL071 (single op-amp) and TL074 (quad op-amp). All capacitors are 4.7 nF and the base resistance is 10 k Ω . An analog 20 MHz oscilloscope on X - Y mode is used

to observe the x - y projections of the attractors experimentally generated by the analogous Chua's circuit.

3.1 Positive parameter space

Considering the parameter variations of α and β in the ranges 14 to 21 and 26 to 38, respectively, the experimental implementation exhibits the sequence of bifurcations presented in Fig. 8. The evolution from periodic to chaotic behavior occurs when α is increased and/or β is decreased, presenting a variety of intermediate topological variations from DC equilibrium through Hopf bifurcations, periodic doubling bifurcations, Rössler-type attractor and double-scroll strange attractor.

The sequence of bifurcations shown in Fig. 9 is obtained varying the parameter α from 19.600 to 28.980 while the parameter β is fixed at 44.170. From a period two orbit, the dynamical behavior of the analogous Chua's circuit evolves to a Rössler-type attractor in the interval of $\alpha = 19.600$ to 21.000. The transition of Rössler to double-scroll occurs at $\alpha = 21.980$. However, there is a window for $\alpha = 24.640$ to

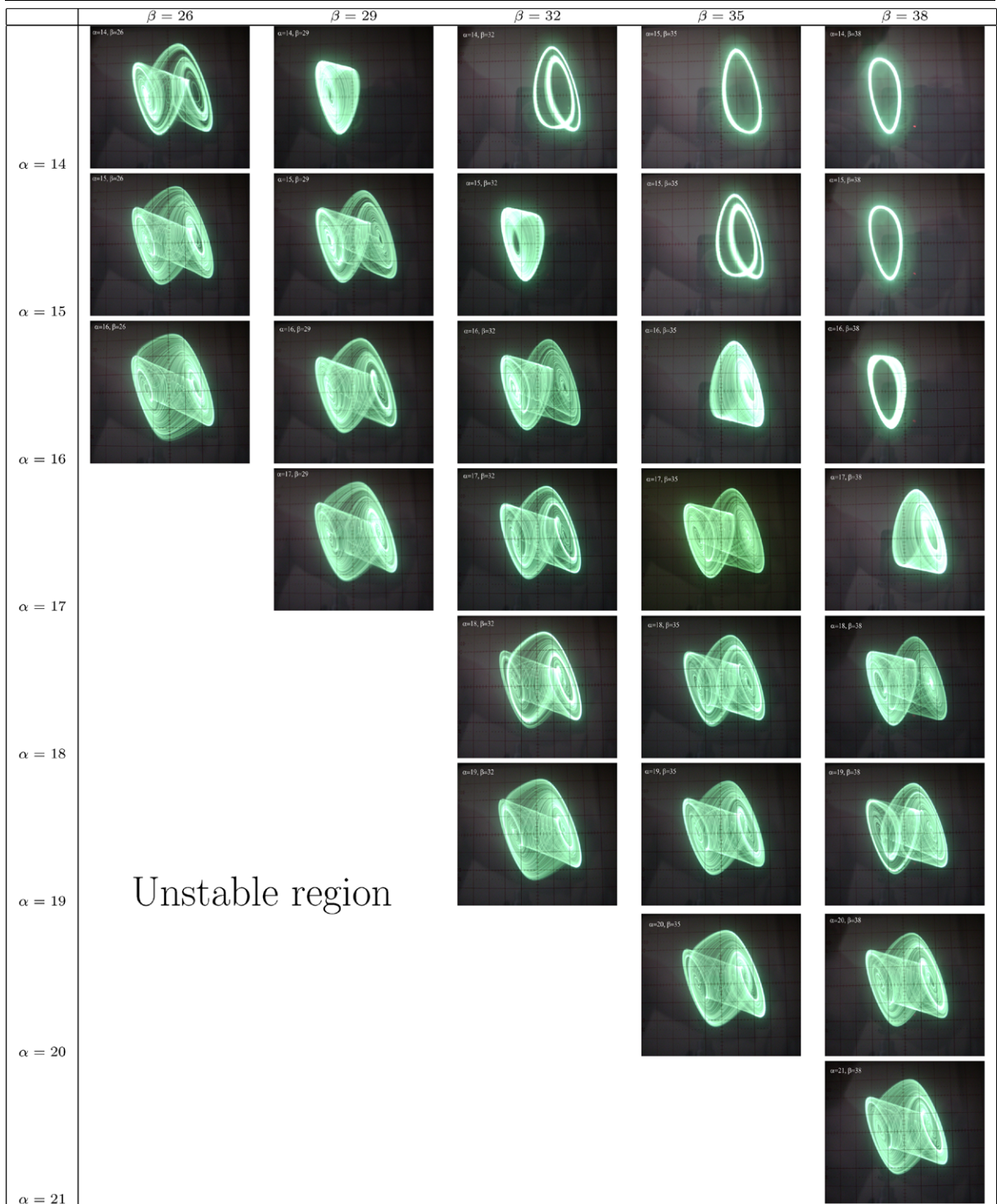


Fig. 8 Experimental mapping of bifurcations in the analogous Chua’s circuit in the ranges $\alpha = 14$ to 21 and $\beta = 26$ to 38 . Attractor projections $(-y) \times (x)$

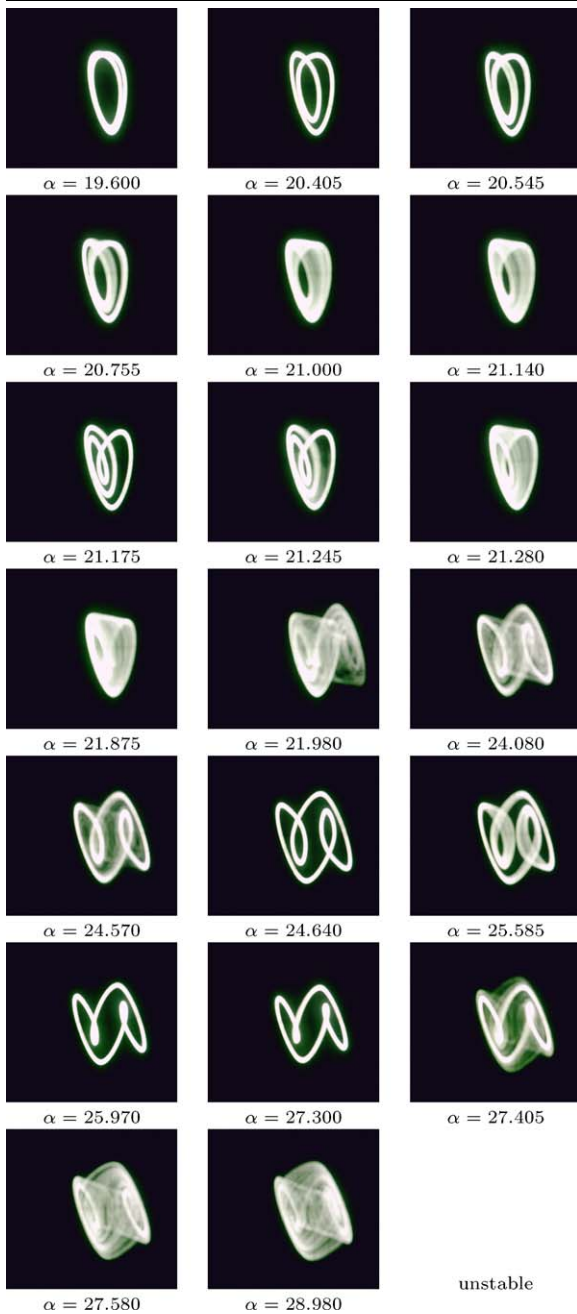


Fig. 9 Experimental sequence of bifurcations in the analogous Chua's circuit: with $\beta = 44.170$, α is varied from 19.600 to 28.980. Attractor projections $(-y) \times (x)$

27.300 where the behavior is periodic. For $\alpha = 27.405$ to 28.980, the dynamics becomes again chaotic and the circuit is unstable for $\alpha > 28.980$.

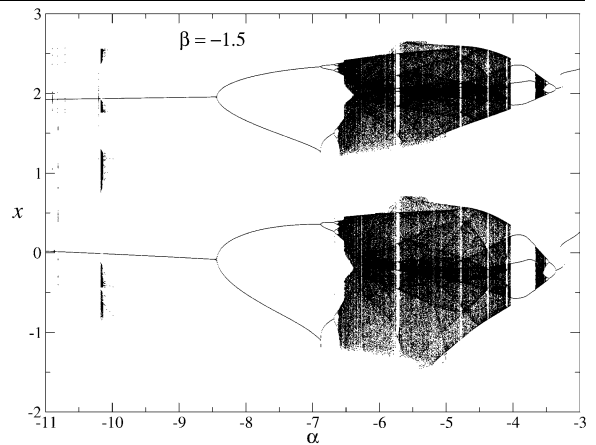


Fig. 10 Bifurcation diagram for the Chua's circuit with negative parameters for fixed $\beta = -1.5$

3.2 Negative parameter space

Although the behavior of the Chua's circuit in the positive parameter space ($\alpha > 0$ and $\beta > 0$) is well known and studied, the dynamics of this circuit with negative parameters ($\alpha < 0$ and $\beta < 0$) has not been sufficiently explored, since this consideration implicates in a physical impossibility: the Chua's circuit would need inductances and/or capacitances with negative values. Since the proposed analogous Chua's circuit is able to sweep the whole parameter space, it can be used for experimental studies of the Chua's system dynamics in the negative parameter space, becoming possible to verify a sequence of new experimental attractors.

In order to verify experimentally this circuit's behavior with negative parameters, a theoretical bifurcation diagram is presented in Fig. 10. This diagram is plotted from the Poincaré maps considering the values of x when the trajectories intercept the plane defined by $y = 0$ with positive dy/dt . These trajectories are evolved from a set of 10 random initial conditions for each parameter, until the system reaches the steady state in order to verify multiple attractors. Since the system dynamics diverge when $\alpha < -11.620$ and $\alpha > -2.324$, the parameter α is swept inside this range while β is maintained at -1.5 . A similarity is observed between the two sets of points in the range $-2 < x < 1$ and in the range $1 < x < 3$, due to a coexistence of attractors. This fact is similar to Rössler-type attractor in the positive parameter space, where there exists a coexistence of two anti-symmetrical attractors ($f(x) = -f(-x)$). According to adopted initial con-

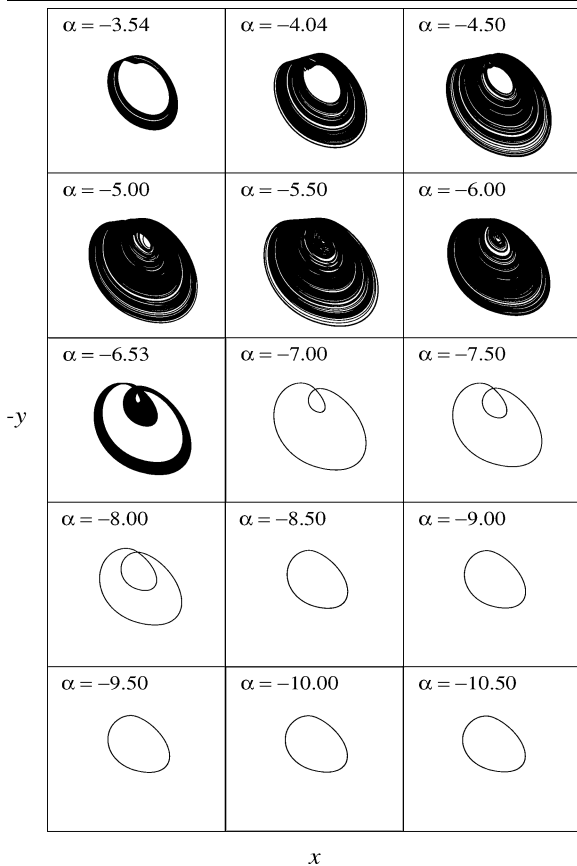


Fig. 11 Sequences of simulated attractors in the Chua's circuit with negative parameters for fixed $\beta = -1.5$. Attractor projections $(-y) \times (x)$

ditions, the system dynamics can converge to one of these stable attractors or diverge to infinity.

The coexistence of attractors is better observed in Fig. 11, where the simulated attractors correspond to bifurcation diagram for $-2 < x < 1$. From $\alpha = -11.5$ to -8.5 , the attractor has period 1 and evolves to period 2 in the range $\alpha = -8.00$ to -7.00 . The system oscillates chaotically from $\alpha = -6.53$ to -3.54 . This route to chaos by period-doubling bifurcations, known as Feigenbaum scenario [23], is experimentally verified in the proposed analogous Chua's circuit, as shown in Fig. 12.

4 Conclusions

This paper presents the design and implementation of an inductor-free realization of the Chua's circuit

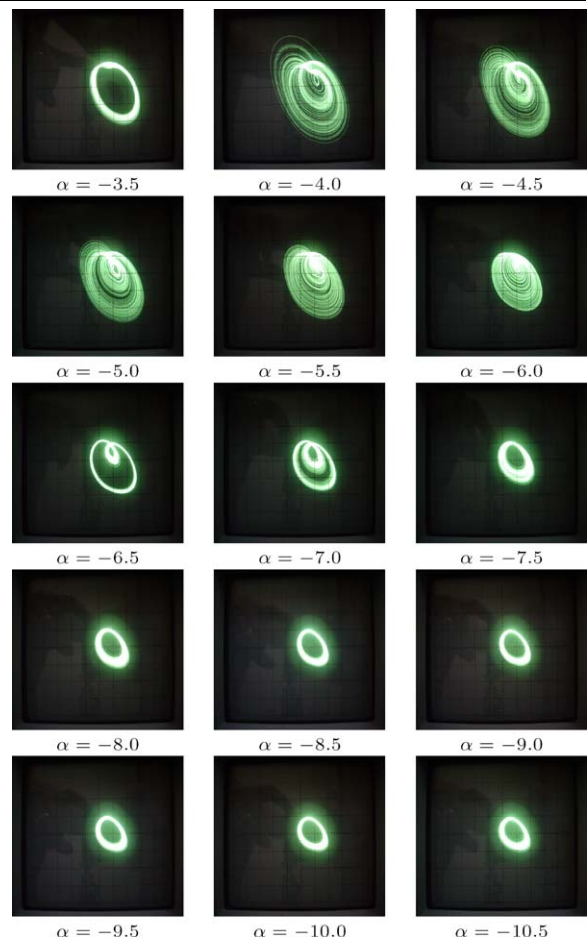


Fig. 12 Sequence of experimental attractors obtained in an analogous Chua's circuit with negative parameters for fixed $\beta = -1.5$. Attractor projections $(-y) \times (x)$

based on the concept of electronic analogy. The proposed analogous Chua's circuit reproduces successfully the dynamical behavior of the Chua's circuit with a remarkable similarity between theoretical simulations (Figs. 2 and 11) and the experimental results (Figs. 6 and 12), providing an accurate, versatile and functional inductor-free implementation of the chaotic Chua's generator. Although the number of components used to implement this analogous circuit is larger than other Chua's oscillator configurations based on VOA, as described in the Table 1, it offers new and interesting features if compared with other alternatives proposed in literature. The three state variables are accessible and explicitly available in the analogous Chua's circuit as voltage signals, whose amplitude can be independently defined in the circuit de-

Table 1 Comparison between inductorless Chua's circuit configurations based on VOA

Configuration	VOA	Diode	Resistor	Capacitor	Total
Kennedy +	3	0	11	3	17
Wien					
Kennedy +	4	0	11	3	18
Girator					
Matsumoto +	2	2	12	3	19
Wien					
Matsumoto +	3	2	12	3	20
Girator					
Analogous	5	2	12	3	22

sign using scaling. Since the dynamics of this analogous Chua's circuit can also be defined in the circuit design, a very slow dynamics can be obtained establishing a large base resistance R instead of an unreliable great integrator electrolytic capacitors C . Since each input resistance of each analog integrator can be substituted by a potentiometer, each coefficient of the coupled equation system (7) can be independently varied in the analogous Chua's circuit, and, in addition, it is easy to adapt the circuit to allow explicit variations of the dimensionless parameters α and β that group all equivalent parameter configurations. The dimensionless parameters α and β can be represented by external DC voltage levels with use of analog multipliers, which makes it easy to execute parameter variations from a computer using an acquisition board with analog outputs. The range of parameter variations in analogous Chua's circuit is very large, allowing also the adoption of negative values for dimensionless parameters α and β . This would be impossible in the Chua's circuit since this implicates in negative inductance or capacitance values. External control inputs can be easily included in the analogous Chua's circuit, introducing new input resistors in the integrators. This circuit can be adapted, to consider the effect of an inductor resistance, introducing a feedback resistor R_{zz} in z -cell. Thus, it is very flexible and allows for the experimental observation of a surprisingly large number of topologically distinct chaotic attractors, if compared with other configurations of the Chua's circuit.

Acknowledgements The authors gratefully acknowledge National Counsel of Technological and Scientific Development (CNPq), State of Minas Gerais Research Foundation (FAPEMIG), State of São Paulo Research Foundation (FAPESP), Gorceix Foundation and Texas Instruments Inc., that contributed to the development of this project.

References

1. Ditto, W., Munakata, T.: Principles and applications of chaotic systems. *Commun. ACM* **38**, 96–102 (1995)
2. Yang, S.-K., Chen, C.-L., Yau, H.-T.: Control of chaos in Lorenz system. *Chaos Solitons Fractals* **13**, 767–780 (2002)
3. Cuomo, K.M., Oppenheim, A.V., Strogatz, S.H.: Synchronization of Lorenz-based chaotic circuits with applications to communications. *IEEE Trans. Circuits Syst. II* **40**, 626–633 (1993)
4. Kiers, K., Schmidt, D., Sprott, J.C.: Precision measurements of a simple chaotic circuit. *Am. J. Phys.* **72**, 503–509 (2004)
5. Madan, R.N.: Chua's Circuit: A Paradigm for Chaos. World Scientific, Singapore (1993)
6. Medrano-T., R.O., Baptista, M.S., Caldas, I.L.: Basic structures of the Shilnikov homoclinic bifurcation scenario. *Chaos* **15**, 33112 (2005)
7. Brown, R.: Generalizations of the Chua equations. *IEEE Trans. Circuits Syst. I* **40**, 878–884 (1993)
8. Matsumoto, T., Chua, L.O., Komuro, M.: The double scroll. *IEEE Trans. Circuits Syst.* **32**, 797–818 (1985)
9. Matsumoto, T., Chua, L.O., Komuro, M.: The double scroll bifurcations. *Int. J. Circuit Theory Appl.* **14**, 117–146 (1986)
10. Zhong, G.O., Ayrom, F.: Experimental confirmation of chaos from Chua's circuit. *Int. J. Circuit Theory Appl.* **13**, 93–98 (1985)

11. Kennedy, M.P.: Robust op-amp realization of Chua's circuit. *Frequenz* **46**, 66–80 (1992)
12. Senani, R., Gupta, S.S.: Implementation of Chua's chaotic circuit using current feedback op-amps. *Electron. Lett.* **34**, 829–830 (1998)
13. Elwakil, A.S., Kennedy, M.P.: Improved implementation of Chua's chaotic oscillator using current feedback op-amp. *IEEE Trans. Circuits Syst. I* **47**, 289–306 (2000)
14. Cruz, J.M., Chua, L.O.: A CMOS IC nonlinear resistor for Chua's circuit. *IEEE Trans. Circuits Syst. I* **39**, 985–995 (1992)
15. Morgül, Ö.: Inductorless realization of Chua's oscillator. *Electron. Lett.* **31**, 1424–1430 (1995)
16. Weldon, T.P.: An inductorless Double Scroll chaotic circuit. *Am. J. Phys.* **58**, 936–941 (1990)
17. Tôrres, L.A.B., Aguirre, L.A.: Inductorless Chua's circuit. *Electron. Lett.* **36**, 1915–1916 (2000)
18. Cruz, J.M., Chua, L.O.: A CMOS IC chip of Chua's circuit. *IEEE Trans. Circuits Syst. I* **40**, 614–625 (1993)
19. Rodriguez-Vazquez, A., Delgado-Restituto, M.: CMOS design of chaotic oscillators using variables: a monolithic Chua's circuit. *IEEE Trans. Circuits Syst. II* **40**, 596–611 (1993)
20. Kiliç, R., Çam, U., Alçi, M., Kuntman, H.: Improved realization of mixed-mode chaotic circuit. *Int. J. Bifurc. Chaos Appl. Sci. Eng.* **12**, 1429–1435 (2002)
21. Kiliç, R.: A comparative study on realization of Chua's circuit: hybrid realizations of Chua's circuit combining the circuit topologies proposed for Chua's diode and inductor elements. *Int. J. Bifurc. Chaos Appl. Sci. Eng.* **13**, 1475–1493 (2003)
22. Rocha, R., Martins Filho, L.S., Machado, R.F.: A methodology for teaching of dynamical systems using analogous electronic circuits. *Int. J. Electr. Eng. Educ.* **43**, 334–345 (2006)
23. Feigenbaum, M.J.: Quantitative universality for a class of nonlinear transformations. *J. Stat. Phys.* **191**, 25–52 (1978)